Senescent epithelial cells remodel the microenvironment for the progression of oral submucous fibrosis through secreting TGF- β 1 (#79139)

First submission

Guidance from your Editor

Please submit by 2 Jan 2023 for the benefit of the authors (and your token reward) .



Structure and Criteria

Please read the 'Structure and Criteria' page for general guidance.



Custom checks

Make sure you include the custom checks shown below, in your review.



Raw data check

Review the raw data.



Image check

Check that figures and images have not been inappropriately manipulated.

Privacy reminder: If uploading an annotated PDF, remove identifiable information to remain anonymous.

Files

Download and review all files from the <u>materials page</u>.

- 5 Figure file(s)
- 1 Table file(s)
- 5 Raw data file(s)
- 14 Other file(s)

Custom checks

Human participant/human tissue checks

- Have you checked the authors ethical approval statement?
- Does the study meet our <u>article requirements</u>?
- Has identifiable info been removed from all files?
- Were the experiments necessary and ethical?

Cell line checks

Is the correct provenance of the cell line described?

Structure and Criteria



Structure your review

The review form is divided into 5 sections. Please consider these when composing your review:

- 1. BASIC REPORTING
- 2. EXPERIMENTAL DESIGN
- 3. VALIDITY OF THE FINDINGS
- 4. General comments
- 5. Confidential notes to the editor
- You can also annotate this PDF and upload it as part of your review

When ready submit online.

Editorial Criteria

Use these criteria points to structure your review. The full detailed editorial criteria is on your guidance page.

BASIC REPORTING

- Clear, unambiguous, professional English language used throughout.
- Intro & background to show context.
 Literature well referenced & relevant.
- Structure conforms to <u>PeerJ standards</u>, discipline norm, or improved for clarity.
- Figures are relevant, high quality, well labelled & described.
- Raw data supplied (see <u>PeerJ policy</u>).

EXPERIMENTAL DESIGN

- Original primary research within Scope of the journal.
- Research question well defined, relevant & meaningful. It is stated how the research fills an identified knowledge gap.
- Rigorous investigation performed to a high technical & ethical standard.
- Methods described with sufficient detail & information to replicate.

VALIDITY OF THE FINDINGS

- Impact and novelty not assessed.

 Meaningful replication encouraged where rationale & benefit to literature is clearly stated.
- All underlying data have been provided; they are robust, statistically sound, & controlled.



Conclusions are well stated, linked to original research question & limited to supporting results.



Standout reviewing tips



The best reviewers use these techniques

Τ	p

Support criticisms with evidence from the text or from other sources

Give specific suggestions on how to improve the manuscript

Comment on language and grammar issues

Organize by importance of the issues, and number your points

Please provide constructive criticism, and avoid personal opinions

Comment on strengths (as well as weaknesses) of the manuscript

Example

Smith et al (J of Methodology, 2005, V3, pp 123) have shown that the analysis you use in Lines 241-250 is not the most appropriate for this situation. Please explain why you used this method.

Your introduction needs more detail. I suggest that you improve the description at lines 57-86 to provide more justification for your study (specifically, you should expand upon the knowledge gap being filled).

The English language should be improved to ensure that an international audience can clearly understand your text. Some examples where the language could be improved include lines 23, 77, 121, 128 – the current phrasing makes comprehension difficult. I suggest you have a colleague who is proficient in English and familiar with the subject matter review your manuscript, or contact a professional editing service.

- 1. Your most important issue
- 2. The next most important item
- 3. ...
- 4. The least important points

I thank you for providing the raw data, however your supplemental files need more descriptive metadata identifiers to be useful to future readers. Although your results are compelling, the data analysis should be improved in the following ways: AA, BB, CC

I commend the authors for their extensive data set, compiled over many years of detailed fieldwork. In addition, the manuscript is clearly written in professional, unambiguous language. If there is a weakness, it is in the statistical analysis (as I have noted above) which should be improved upon before Acceptance.



Senescent epithelial cells remodel the microenvironment for the progression of oral submucous fibrosis through secreting TGF- $\beta1$

Zijia Wang ¹, Ying Han ¹, Ying Peng ¹, Shuhui Shao ¹, Huanquan Nie ¹, Kun Xia ², Haofeng Xiong ^{1,3,4,5}, Tong Su ^{Corresp.}

Corresponding Author: Tong Su Email address: sutong@csu.edu.cn

Objectives: Cellular senescence is strongly associated with fibrosis and tumorigenesis. However, whether the epithelium of oral submucous fibrosis (OSF) undergoes premature senescence remains unclear. This study investigates the roles of senescent epithelial cells in OSF. Methods: The immunohistochemistry and Sudan black B staining were performed to identify epithelium senescence in OSF tissues. Arecoline was used to induce human oral keratinocytes (HOKs) senescence. The cell morphology, senescence-associated β galactosidase activity, cell counting Kit 8, immunofluorescence, quantitative real-time PCR, and western blot assay were used to identification of senescent HOKs. The enzyme-linked immunosorbent assay was exerted to evaluate the levels of transforming growth factor \$1 (TGF-β1) in the supernatants of HOKs treated with or without arecoline. **Results:** The senescence-associated markers, p16 and p21, were overexpressed in OSF epithelium. These expressions were correlated with alpha-smooth actin (α -SMA) positively and proliferating cell nuclear antigen (PCNA) negatively. Moreover, Sudan black staining showed that there was more lipofuscin in OSF epithelium. In vitro, HOKs treated with arecoline showed senescence-associated characteristics including enlarged and flattened morphology, senescence-associated β galactosidase staining, cell growth arrest, γH2A.X foci, upregulation of p53, p21, and TGF-β1 protein levels. Moreover, senescent HOKs secreted more TGF-β1. **Conclusions:** Senescent epithelial cells are involved in OSF progression and may become a promising target for OSF treatment.

¹ Department of Oral and Maxillofacial Surgery, Center of Stomatology, Xiangya Hospital, Central South University, Changsha, Hunan, China

² Center for Medical Genetics & Hunan Key Laboratory of Medical Genetics, School of Life Sciences, Central South University, Changsha, Hunan, China

Research Center of Oral and Maxillofacial Tumor, Xiangya Hospital, Central South University, Changsha, China

⁴ Institute of Oral Precancerous Lesions, Central South University, Changsha, China

⁵ National Clinical Research Center for Geriatric Disorders, Xiangya Hospital, Changsha, China





Senescent epithelial cells remodel the microenvironment for the progression of oral submucous 1 2 fibrosis through secreting TGF-β1 3 4 Zijia Wang¹, Ying Han¹, Ying Peng ¹, Shuhui Shao¹, Huanquan Nie¹, Kun Xia⁵, Haofeng Xiong^{1, 2, 3, 4, *}, Tong 5 Su^{1, 2, 3, 4, *} 6 7 1. Department of Oral and Maxillofacial Surgery, Center of Stomatology, Xiangya Hospital, Central South 8 University, Changsha, Hunan, 410008, China 9 2. Research Center of Oral and Maxillofacial Tumor, Xiangya Hospital, Central South University, 10 Changsha, Hunan, 410008, China 11 3. Institute of Oral Precancerous Lesions, Central South University, Changsha, Hunan, 410008, China 12 4. National Clinical Research Center for Geriatric Disorders, Xiangya Hospital, Changsha, Hunan, 410008, 13 China 14 5. Center for Medical Genetics & Hunan Key Laboratory of Medical Genetics, School of Life Sciences, 15 Central South University, Changsha, Hunan, 410008, China 16 17 *Corresponding author: Tong Su, M.D., Department of Oral and Maxillofacial Surgery, Center of 18 Stomatology, Xiangya Hospital, Central South University, NO.87 Xiangya Road, Changsha, Hunan, 19 410008, China (email: sutong@csu.edu.cn); Haofeng Xiong, Center of Stomatology, Xiangya Hospital, 20 Central South University, NO.87 Xiangya Road, Changsha, Hunan, 410008, China (email: 21 xionghaofeng@sklmg.edu.cn) 22 23



PeerJ

24	A1	ostr	act

- 25 **Objectives:** Cellular senescence is strongly associated with fibrosis and tumorigenesis. However,
- 26 whether the epithelium of oral submucous fibrosis (OSF) undergoes premature senescence remains
- 27 unclear. This study investigates the roles of senescent epithelial cells in OSF.
- 28 Methods: The immunohistochemistry and Sudan black B staining were performed to identify
- 29 epithelium senescence in OSF tissues. Arecoline was used to induce human oral keratinocytes (HOKs)
- 30 senescence. The cell morphology, senescence-associated β galactosidase activity, cell counting Kit 8,
- 31 immunofluorescence, quantitative real-time PCR, and western blot assay were used to identification
- 32 of senescent HOKs. The enzyme-linked immunosorbent assay was exerted to evaluate the levels of
- 33 transforming growth factor β 1 (TGF- β 1) in the supernatants of HOKs treated with or without
- 34 arecoline.
- 35 **Results:** The senescence-associated markers, p16 and p21, were overexpressed in OSF epithelium.
- 36 These expressions were correlated with alpha-smooth actin (α -SMA) positively and proliferating cell
- 37 nuclear antigen (PCNA) negatively. Moreover, Sudan black staining showed that there was more
- 38 lipofuscin in OSF epithelium. In vitro, HOKs treated with arecoline showed senescence-associated
- 39 characteristics including enlarged and flattened morphology, senescence-associated β galactosidase
- 40 staining, cell growth arrest, γH2A.X foci, upregulation of p53, p21, and TGF-β1 protein levels.
- 41 Moreover, senescent HOKs secreted more TGF-β1.
- 42 **Conclusions:** Senescent epithelial cells are involved in OSF progression and may become a promising
- 43 target for OSF treatment.

44

- 45 **Keywords:** Oral submucous fibrosis, epithelial cell, cellular senescence, senescence-associated
- 46 secretory phenotype, transforming growth factor β1



1. Introduction

Oral submucous fibrosis (OSF) is a premalignant mucosal disease with inflammation and progressive fibrosis. With fibrosis progresses, it can severely impair oral functions, such as eating, speaking, and swallowing. Moreover, 1.5-15% of OSF may eventually develop into oral squamous cell carcinoma (OSCC).¹ Despite many current OSF treatments being efficient, they only relieve symptoms. Therefore, it is urgent to find a potent therapy for OSF to reverse or even block its progression and malignant transformation.

Numerous studies have shown that cellular senescence is closely related to fibrosis and cancer.^{2,3} Senescent cells exhibit cell cycle arrest and develop a secretory profile composed of growth factors, inflammatory cytokines, chemokines, and other bioactive molecules, termed the senescence-associated secretory phenotype (SASP).⁴ Cell cycle arrest prevents damaged cells from proliferating, and the secretion of SASP recruits immune cells to eliminate senescent cells, making cellular senescence a critical protective mechanism.⁵ Senescent cells, however, have a detrimental effect on neighboring cells by generating excessive SASP when they abnormally accumulate in tissues.⁶ For example, senescent alveolar type II cells contributed to lung fibrogenesis by activating the profibrotic phenotype of alveolar macrophages through secreting SASP.⁷ Through SASP, senescent hepatic stellate cells enhanced hepatocellular carcinoma cell growth and accelerated xenograft tumor growth.⁸ Besides, senotherapy, which targets senescent cells, has been demonstrated that is an effective treatment for fibrosis and cancer.⁹ However, the mechanism of cellular senescence in OSF is still poorly understood.

There has been relatively little study on cellular senescence in OSF so far. Rehman et al. reported that senescent fibroblasts remodel the tissue microenvironment to promote the progression of OSF to OSCC through releasing SASP.¹⁰ However, as the first barrier, far too little attention has been paid to the roles of the epithelium in the pathogenesis of OSF. Since epithelial atrophy is a characteristic pathological manifestation of OSF and OSCC originates from the epithelium, we speculated that epithelial cells of OSF may undergo premature senescence, which participates in OSF progression.

In this study, we demonstrated that OSF epithelial cells undergo premature senescence and could play roles in OSF progression.



2. Materials and methods

2.1 Patient samples

A total of 30 samples were collected from the center of stomatology, Xiangya Hospital from September 2019 to May 2020. 21 OSF tissues were obtained from OSF patients without OSF therapy. 9 normal oral mucosa (NOM) samples were obtained from healthy volunteers during surgical removal of the lower third molars. All samples were diagnosed by pathological examination based on the 2005 World Health Organization classification system. All research subjects gave written informed consent in accordance with the Helsinki Declaration. This study was approved by the Medical Ethics Committee of Xiangya Hospital, Central South University (ethics approval number 201803795).

2.2 Immunohistochemistry assay

The immunohistochemistry was performed as described previously.¹¹ The following primary antibodies were used in immunohistochemistry: p16 (1:500, ab108349, Abcam), p21 (1:50, 2947T, Cell signaling technology, CST), alpha-smooth actin (α -SMA) (1:200, ab5694, Abcam), proliferating cell nuclear antigen (PCNA) (1:16000, 2586S, CST). Phosphate-buffered saline (PBS) was used instead of the primary antibody as a negative control, and NOM tissues were used as a positive control. All slides were observed by microscopy (Leica Microsystems, Cambridge, UK). The staining results were quantitatively evaluated using the Image-Pro-Plus 5.0 software to measure the mean optical density (MOD) of positive p16, p21, PCNA, and α -SMA in OSF tissues (MOD = integral optical density (IOD)/area of interest). The epithelium or subepithelial areas of NOM and OSF tissues were marked as the interest areas for analysis.

2.3 Sudan black B staining

To detect lipofuscin accumulation in OSF epithelium, Sudan black B solution was used to stain the lipofuscin. Sudan black B staining (S109070, Aladdin) was carried out as described previously.¹²

2.4 Cell lines and cell culture

Human Oral Keratinocytes (HOKs) is currently the only normal oral epithelial cell line available, which were gifted by Professor Sun Zhijun from the school of Stomatology, Wuhan University. Its culture method was as previously described.¹³ As the major components of betel nut, we used arecoline to induce HOKs senescence. HOKs were randomly divided into 6 groups, and after starvation in serum-free medium overnight, they were incubated with complete medium containing different concentrations of arecoline (0, 20, 40, 80, 160, and 320 µg/ml) for 24h. Then, all groups were replaced with complete medium, and the medium was changed every 3 days for 10-14 days.

2.5 Induction of HOKs senescence by arecoline

To confirm the roles of senescent epithelial cells, we used arecoline to induce HOKs senescence. The cells were randomly divided into 6 groups and treated with different concentrations of arecoline (0, 20, 40, 80, 160, and 320 μ g/ml). After starving overnight in serum-free medium, the cells were incubated with medium at different concentrations of arecoline for 24h. Then, the mediums were replaced with OKM every 3 days for 10-14 days.



2.6 Senescence-associated β galactosidase (SA- β -gal) activity assay

The SA- β -gal activity was performed using a SA- β -gal staining Kit (CS0030, Sigma-Aldrich) and by following the manufacturer's instructions. Briefly, HOKs after senescence induction were seeded into 24-well culture plates at 1×10⁴ cells per well. The next day, the cells were washed three times with PBS and fixed by cell fixative solution in the SA- β -gal staining Kit for 7 min at room temperature. Then, the cells were washed three times with PBS to remove the solution. The staining mixture containing X-gal prepared following the instruction was incubated with the cells in a regular incubator at 37°C overnight without CO₂. The cells were observed by microscopy (Leica Microsystems, Cambridge, UK). A total of 5 fields in each group were selected under the microscope and the total cells and SA- β -gal positive cells in each field were counted by ImageJ 5.0. The proportion of SA- β -gal positive cells was obtained by calculating the ratio of the average SA- β -gal positive cell number to the average total cell number in each group.

2.7 Immunofluorescence assay

Immunofluorescence was applied to examine the expression of phosphor-histone H2A.X (γ H2A.X) in HOKs treated with different concentrations of arecoline. After senescence induction, the cells were seeded into 24-wells culture plates at 1×10^4 per well. The next day, the cells were fixed with 4% paraformaldehyde for 10 min. Subsequently, the cells were permeabilized with 0.1% Triton X-100 solution and blocked with goat serum (ZLI-9056, ZSGB-BIO). After PBS washing, the cells were incubated with monoclonal rabbit anti- γ H2A.X (1:400, 9718, CST) at 4°C overnight. The next day, the cells were incubated with cy3-conjugated secondary antibody (AP132C, Sigma) for 1 h in dark, and then counterstained with DAPI (C1002, Beyotime) at room temperature for 1 min. Immunofluorescence images were acquired using a fluorescence microscope (Leica Microsystems, Cambridge, UK). A total of 5 fields in each group were selected under the microscope and the total cells and γ H2A.X positive cells in each field were counted by ImageJ 5.0. The proportion of γ H2A.X positive cells was obtained by calculating the ratio of the average γ H2A.X positive cell number to the average total cell number in each group.

2.8 Cell proliferation assay

Cell proliferation ability was assessed by Cell Counting Kit 8 (CCK8). CCK8 assay was performed by the manufacturer's protocol (A311-01, Vazyme). After senescence induction, HOKs were seeded into 96-well plates at a density of 5000 cells per well and continually cultured for 0, 24, 48, 72, and 96 h. Then, CCK8 solution (10 μ L) was added to each well for 2 h incubation at 37°C. The plates were detected at the indicated time (0, 24, 48, 72, and 96 h) using a microplate reader (Synergy 2, Biotek) at a wavelength of 450 nm.

2.9 Quantitative reverse transcription polymerase chain reaction (qRT-PCR) assay

Total RNA was extracted from HOKs treated with different concentrations of arecoline using TRIzol reagent (Invitrogen). The total RNA was reverse transcribed to cDNA using RevertAid™ Master Mix, with DNase I Kit (M16325, Thermo Scientific) according to the manufacturer's protocol.



159 qPCR was performed using Maxima SYBR Green qPCR Master Mix (K0252, Thermo Scientific) on a Real-Time PCR Detection System (CFX96, Bio-Rad) according to the manufacturer's protocol. All 160 qPCR primers were listed in Table 1. The relative mRNA expression was calculated using the 2-ΔΔCt 162 method.

163 164

165

166 167

168

169

170

171 172

173

174

175

176

161

2.10 Western blotting assay

The total protein was extracted from HOKs treated with different concentrations of arecoline using SDS lysis buffer (P0013G, Beyotime). The total protein concentration was detected using PierceTM BCA Protein Assay Kit (23225, Thermo Fisher Scientific). A total of 40 µg protein was added to 10% polyacrylamide gel and transferred to polyvinylidene fluoride (PVDF) membranes. The membranes were blocked with 5% skim milk for 1 hour at room temperature. After PBST washing three times, the membranes were incubated with primary antibodies overnight at 4°C overnight: p16 (1:2000, ab108349, Abcam), p21 (1:2000, 2946, CST), p53 (1:1000, 48818, CST), transforming growth factor β1 (TGF-β1) (1:1000, ab215715, Abcam), and GAPDH (1:1000, 5174T, CST). Then, the membranes were incubated with the corresponding horseradish peroxidase-conjugated secondary antibodies (anti-Rabbit/mouse 1:5000~10000) for 1 hour at room temperature. The membranes were developed using SuperSignal™ West Pico PLUS chemiluminescent substrate (34580, Thermo Fisher Scientific) and detected by a chemiluminescent imaging system (MiniChemi 610, Sagecreation). and analyzed using the ImageJ 5.0 version software.

177 178 179

180

181

182

2.11 Enzyme-linked immunosorbent (Elisa) assay

Levels of TGF-β1 in supernatants were measured by the Human TGF-β1 Elisa Kit (PT880, Beyotime) following the manufacturer's protocol. The absorbance of samples was detected at 450 nm using a microplate reader (Synergy 2, Biotek). The TGF-β1 concentration of each sample was determined by a standard curve provided from the manufacturer's protocol.

183 184 185

186

187

188

189

2.12 Statistical analysis

All experiments were conducted in triplicate and repeated at least 3 times. All data were shown as mean ± standard deviation. Continuous variables were assessed by the student's t test or Mann-Whitney U test according to the normality test. Spearman's correlation was used to analyze the correlation. P value < 0.05 was considered statistically significance. Statistical analysis was performed using SPSS 24.0 software.



3. Results

3.1 The epithelium of OSF undergoes premature senescence

p16 and p21 belong to cyclin-dependent kinase inhibitors, which are major drivers of the cycle arrest in senescence and have been confirmed to be one of the defining features of senescent cells. ¹⁴ Therefore, we detected the expressions of p16 and p21 in the epithelium of OSF and normal tissues. We found that p16 and p21 were overexpressed in OSF epithelium compared with the normal epithelium (Figure 1A-D). In contrast, PCNA was highly expressed in the epithelium of NOM (Figure 1A, B, E). Moreover, the expressions of p16 and p21 were negatively correlated with PCNA in OSF epithelial tissues (Figure 1H-K).

To further confirm epithelial cells senescence in OSF, we detected the accumulation of lipofuscin in OSF epithelium. Lipofuscin is abnormally accumulated in senescent cells, another well-established senescence marker.¹² After Sudan black B staining, we found that the lipofuscin was widely distributed in OSF epithelium (Figure 1G).

3.2 Correlation between the epithelial cell senescence and myofibroblast activation in human OSF tissues

To further study the correlation between the epithelial cell senescence and myofibroblast activation in OSF tissue, we detected the expression of α -SMA that is a characteristic marker of myofibroblast activation. We observed that there were α -SMA positive spindle cells located in the lamina propria adjacent to the epithelium of OSF (Figure 1B). In sharp contrast, we only detected rings of α -SMA positive cells representing blood vessels in the lamina propria of normal tissues (Figure 1A). We hardly found the α -SMA positive spindle cells in normal tissues. Moreover, the expression of α -SMA in OSF tissues was extremely higher than in normal tissues (p<0.001, Figure 1F). Further analysis revealed that α -SMA expression in OSF tissues was positively correlated with the expressions of senescence markers, p21 and p16 (p<0.01, Figure 1H).

3.3 Arecoline induced senescence-like cell morphology and suppressed cell proliferation in HOKs

HOK is the immortalized epithelial cell from the basal layer of oral mucosa tissues. Thus, we selected it to validate the roles of senescent epithelial cells. Since OSF is an oral mucosal disease associated with the chewing of areca nut, we choose arecoline to induce HOKs senescence due to it is a major component of areca nut. To confirm HOKs developing senescence, we examined senescence-associated phenotypes in HOKs.

After HOKs were treated with different concentrations of arecoline for 24h, they gradually appeared an enlarged and flattened morphology, following another 5-7 days of culture (Figure 2A). Meanwhile, the enlarged and flattened HOKs also showed SA-β-gal positive staining (Figure 2A). The proportion of SA-β-gal positive HOKs was gradually increased with arecoline concentration. Among different concentrations of arecoline, the 320 μg/ml group had the highest proportion of SA-β-gal positive HOKs compared with other groups (p < 0.05, Figure 2B). Moreover, the surface area of SA-β-gal positive cells was about 10-fold more than that of SA-β-gal negative cells (p < 0.05, Figure 2C). CCK8 assay showed that compared with that of other groups, the proliferation ability of the 320 μg/ml group was largely suppressed after senescence induction (p < 0.05, Figure 2D).



3.4 Arecoline induced DNA damage response (DDR) in HOKs

The phosphorylated-histone H2A was detected in HOKs after senescence induction, a hallmark of DNA double-strand breakage in cells, because DNA damage stimulates DNA damage response (DDR) that triggers senescence. ^{15,16} We found that γ H2A.X was mainly detected in HOKs treated with high concentrations of arecoline (160 and 320 μ g/ml) (Figure 3A). The proportion of γ H2A.X positive HOKs was elevated with arecoline concentration, and that in the 320 μ g/ml group was significantly higher than in other groups (p<0.05, Figure 3B). Moreover, we observed that γ H2A.X was mainly expressed in the nucleus of the enlarged and flatted HOKs (Figure 3C).

3.5 Arecoline-induced HOK senescence was associated with p53/p21 pathway

Cell cycle arrest of senescent cells is controlled by activation of the p53/p21 or p16/Rb pathway. ¹⁶ Since most of HOKs in the 320 μ g/ml group undergo senescence, we compared the levels of p16, p21, and p53 between the groups of the normal control (0 μ g/ml) and the 320 μ g/ml. We found that p21 expression was dramatically upregulated at the protein and mRNA level (p < 0.01, Figure 4A, B), while p53 expression was on the rise only at the protein level in the 320 μ g/ml group (p < 0.05, Figure 4A, C). No difference was observed in p16 at protein and mRNA levels in both groups (Figure 4A).

3.6 The synthesis and secretion of TGF-β1 are increased in senescent HOKs

Growth factors are a prominent constituent of SASP. Given that TGF- $\beta1$ is a well-known profibrotic factor, we examined the levels of TGF- $\beta1$ at protein and mRNA between the groups of the normal control (0 μ g/ml) and the 320 μ g/ml. The levels of TGF- $\beta1$ in the 320 μ g/ml group were all significantly upregulated at protein and mRNA, compared with the normal control group (p<0.05, Figure 4D). In addition, although the density of HOKs in the 320 μ g/ml group after senescence induction was approximately 30-40% of that in the normal control group, we found that the levels of TGF- $\beta1$ in the supernatant of the 320 μ g/ml group were increased approximately 2-fold compared to the control group (p<0.01, Figure 4E).



263264

265

266267

268

269

270

271

272

273274

275

276

277278

279

280281

282

283

284

285

286

287

288289

290

291

292293

294

295

296

297

298

299

300301

Discussion

The treatments of OSF are currently used to effectively control symptoms and improve oral functions and the life quality of OSF patients.¹ However, these treatments can neither completely cure OSF nor block its transformation to OSCC. Senescent cells have recently been shown to be involved in the development of fibrosis diseases and tumors,^{2,3} and targeting senescent cells can effectively suppress their progression.⁹ To our knowledge, our work is the first to focus and study cellular senescence in the epithelium of OSF.

In the present study, we found that lipofuscin was abnormally increased in OSF epithelium. Additionally, the expressions of p16 and p21 were elevated in the epithelium of OSF by immunohistochemistry assay. Their expressions were negatively correlated to PCNA expression, which was hardly expressed in the epithelium of OSF. p16 and p21 both are well-established markers of cellular senescence and belong to the Cyclin-Dependent Kinase Inhibitor family, mediating cell cycle arrest to suppress cell proliferation. These results provided evidence that the epithelium of OSF undergoes cellular senescence, suggesting that the epithelial senescence contributes to epithelial atrophy of OSF. Meanwhile, we also found that p16 and p21 expression were positively correlated with α -SMA expression, a marker of the activated myofibroblast. Activated myofibroblasts are the major source of collagen in fibrosis. These results indicated that the epithelial senescence was associated with the myofibroblast activation. Tian et al. have confirmed that senescent alveolar epithelial cells activated myofibroblasts through intercellular communication in lung fibrosis. These findings implied that senescent epithelial cells could activate myofibroblasts by intercellular communication. Therefore, to further investigate the roles of senescent epithelial cells, we used are coline to induce HOKs senescence in vitro.

Arecoline has been shown to generate reactive oxygen species (ROS) in different types of cells, 19,20 and ROS is one of the common triggers of cellular senescence. 15 We found that HOKs exhibited various senescence-associated phenotypes under the short-duration stimulation of arecoline. The proportion of these cells showed a dose-dependent relationship with arecoline. A possible explanation for this might be that are coline raised intracellular reactive oxygen species (ROS) levels in a dosedependent manner.²¹ Moreover, yH2A.X foci localized in the nucleus of senescent-like cells, and the expressions of p53 and p21 were obviously higher in HOKs treated with 320 µg/ml arecoline than in HOKs without arecoline. The formation of γH2A.X foci represents the activation of DNA damage response (DDR) and dysregulation of the cell cycle.²² The DDR can activate the p53/p21 pathway, and p21 is responsible for initiating senescence.¹⁵ These findings suggested that arecoline can induce HOKs senescence, which is consistent with the study of Patil et al..²³ However, our study also provided an insight that are coline-induced senescence in HOKs is closely linked to the p53/p21 pathway. In addition, TGF-β1 expressions were significantly increased at protein and mRNA levels in HOKs treated with 320 µg/ml arecoline, compared with HOKs without arecoline. These results indicated that senescent HOKs can synthesize more TGF-β1. Although TGF-β1 is one of the common components of SASP, the composition of SASP depends on cell type and stimulus. Subsequently, we examined TGF-β1 levels in the supernatant to determine that senescent HOKs can secrete excessive

As identified in Elisa experiments, we found that secreted TGF-β1 levels in senescent HOKs





supernatants were approximately 2-fold higher than in normal HOKs supernatants. These results suggested that senescent HOKs could release excessive TGF- β 1. Our previous study reported that TGF- β 1 was overexpressed in the epithelium of OSF. Consequently, senescent epithelial cells could be one of the major cellular source of upregulated TGF- β 1 in the epithelium of OSF.

As a pleiotropic cytokine, firstly, TGF- β 1 has been demonstrated to induce myofibroblasts differentiation to facilitate fibrosis, ²⁴⁻²⁶ and secondly, TGF- β 1 can participate in tumorigenesis by mediating epithelial-mesenchymal transition, immunosuppression, and stemness. ^{27,28} Moreover, Rana et al. have demonstrated that TGF- β 1 can induce senescence in mouse alveolar type II cells. ⁷ Hence, it raises the possibility that there may be a paracrine positive-feedback loop to amplify senescence and reinforce TGF- β 1 signaling in OSF epithelium.

Accordingly, targeting the senescent epithelial may constitute a promising therapeutic approach for OSF. Amor et al. recently reported in Nature that chimeric antigen receptor T cells can effectively eliminate senescent cells, which extend the lifespan of mice harboring lung adenocarcinoma and restore tissue homeostasis in mice with liver fibrosis.⁹

In summary, we found that the epithelium of OSF undergoes premature senescence, and there is a positive correlation between senescent epithelial cells and myofibroblasts activation. In addition, our study indicated that senescent HOKs secrete excessive TGF- β 1, which indicated that senescent epithelial cells could affect surrounding cells by TGF- β 1 secretion. Moreover, this research has an important implication for developing targeted therapeutics for senescent epithelial cells in OSF, which may be beneficial for reversing and blocking its progression and malignant transformation.



PeerJ

323	Conflict of interest
324	We have no conflicts of interest.
325	
326	Acknowledgements
327	We thank Professor Sun Zhijun in Hospital of Stomatology Wuhan University for supporting HOKs.
328	This work was supported by the National Natural Science Foundation (81873717 and 82170973) and
329	the Clinical Research Fund of the National Clinical Research Center for Geriatric Disorders of Xiangya
330	Hospital (2021LNJJ08).



- 332 Reference
- 333 1. Shih YH, Wang TH, Shieh TM, Tseng YH. Oral Submucous Fibrosis: A Review on Etiopathogenesis, Diagnosis, and Therapy. *Int J Mol Sci.* 2019;20(12).
- Yao C, Guan X, Carraro G, et al. Senescence of Alveolar Type 2 Cells Drives Progressive Pulmonary
 Fibrosis. *Am J Respir Crit Care Med.* 2021;203(6):707-717.
- 337 3. Huang Y, Yang X, Meng Y, et al. The hepatic senescence-associated secretory phenotype promotes
- hepatocarcinogenesis through Bcl3-dependent activation of macrophages. *Cell Biosci.* 2021;11(1):173.
- Shmulevich R, Krizhanovsky V. Cell Senescence, DNA Damage, and Metabolism. *Antioxid Redox* Signal. 2021;34(4):324-334.
- 342 5. Herranz N, Gil J. Mechanisms and functions of cellular senescence. *J Clin Invest*. 2018;128(4):1238-343 1246.
- Loo TM, Miyata K, Tanaka Y, Takahashi A. Cellular senescence and senescence-associated secretory phenotype via the cGAS-STING signaling pathway in cancer. *Cancer Sci.* 2020;111(2):304-
- 346 311.
- 7. Rana T, Jiang C, Liu G, et al. PAI-1 Regulation of TGF-β1-induced Alveolar Type II Cell Senescence,
- SASP Secretion, and SASP-mediated Activation of Alveolar Macrophages. *Am J Respir Cell Mol Biol.* 2020;62(3):319-330.
- Li F, Huangyang P, Burrows M, et al. FBP1 loss disrupts liver metabolism and promotes tumorigenesis through a hepatic stellate cell senescence secretome. *Nat Cell Biol.* 2020;22(6):728-739.
- 352 9. Amor C, Feucht J, Leibold J, et al. Senolytic CAR T cells reverse senescence-associated pathologies.
 353 Nature. 2020;583(7814):127-132.
- Rehman A, Ali S, Lone MA, et al. Areca nut alkaloids induce irreparable DNA damage and senescence in fibroblasts and may create a favourable environment for tumour progression. *J Oral*
- 356 Pathol Med. 2016;45(5):365-372.
- 357 11. Min A, Xiong H, Wang W, et al. CD147 promotes proliferation and migration of oral cancer cells by inhibiting junctions between E-cadherin and β-catenin. *J Oral Pathol Med.* 2020;49(10):1019-1029.
- 359 12. Georgakopoulou EA, Tsimaratou K, Evangelou K, et al. Specific lipofuscin staining as a novel 360 biomarker to detect replicative and stress-induced senescence. A method applicable in cryo-361 preserved and archival tissues. *Aging (Albany NY)*. 2013;5(1):37-50.
- Wang W, Xiong H, Hu Z, et al. Experimental study on TGF-β1-mediated CD147 expression in oral
 submucous fibrosis. *Oral Dis.* 2018;24(6):993-1000.
- 364 14. Calcinotto A, Kohli J, Zagato E, Pellegrini L, Demaria M, Alimonti A. Cellular Senescence: Aging, Cancer, and Injury. *Physiol Rev.* 2019;99(2):1047-1078.
- 366 15. Di Micco R, Krizhanovsky V, Baker D, d'Adda di Fagagna F. Cellular senescence in ageing: from mechanisms to therapeutic opportunities. *Nat Rev Mol Cell Biol.* 2021;22(2):75-95.
- 368 16. Gorgoulis V, Adams PD, Alimonti A, et al. Cellular Senescence: Defining a Path Forward. *Cell.* 2019;179(4):813-827.
- Lee YH, Liao YW, Lu MY, Hsieh PL, Yu CC. LINC00084/miR-204/ZEB1 Axis Mediates
 Myofibroblastic Differentiation Activity in Fibrotic Buccal Mucosa Fibroblasts: Therapeutic Target
- for Oral Submucous Fibrosis. *J Pers Med.* 2021;11(8).



Manuscript to be reviewed

- Tian Y, Li H, Qiu T, et al. Loss of PTEN induces lung fibrosis via alveolar epithelial cell senescence
 depending on NF-κB activation. *Aging Cell*. 2019;18(1):e12858.
- 375 19. Shih YH, Chiu KC, Wang TH, et al. Effects of melatonin to arecoline-induced reactive oxygen 376 species production and DNA damage in oral squamous cell carcinoma. *J Formos Med Assoc.* 377 2021;120(1 Pt 3):668-678.
- Shih LJ, Wang JY, Jheng JY, et al. Betel Nut Arecoline Induces Different Phases of Growth Arrest
 between Normal and Cancerous Prostate Cells through the Reactive Oxygen Species Pathway. *Int I Mol Sci.* 2020;21(23).
- Yen CY, Lin MH, Liu SY, et al. Arecoline-mediated inhibition of AMP-activated protein kinase through reactive oxygen species is required for apoptosis induction. *Oral Oncol.* 2011;47(5):345-351.
- 383 22. Hernandez-Segura A, Nehme J, Demaria M. Hallmarks of Cellular Senescence. *Trends Cell Biol.* 384 2018;28(6):436-453.
- Patil S, Sarode SC, Ashi H, et al. Triphala extract negates are coline-induced senescence in oral mucosal epithelial cells in vitro. *Saudi J Biol Sci.* 2021;28(4):2223-2228.
- 387 24. Huang Y, Xie Y, Abel PW, et al. TGF-β1-induced miR-424 promotes pulmonary myofibroblast
 388 differentiation by targeting Slit2 protein expression. *Biochem Pharmacol.* 2020;180:114172.
- Little K, Llorián-Salvador M, Tang M, et al. Macrophage to myofibroblast transition contributes to subretinal fibrosis secondary to neovascular age-related macular degeneration. *J Neuroinflammation*. 2020;17(1):355.
- Zhang B, Gao L, Shao C, Deng M, Chen L. Arecoline Enhances Phosphodiesterase 4A Activity to
 Promote Transforming Growth Factor-β-Induced Buccal Mucosal Fibroblast Activation via cAMP Epac1 Signaling Pathway. Front Pharmacol. 2021;12:722040.
- Cave DD, Di Guida M, Costa V, et al. TGF-β1 secreted by pancreatic stellate cells promotes
 stemness and tumourigenicity in pancreatic cancer cells through L1CAM downregulation.
 Oncogene. 2020;39(21):4271-4285.
- 398 28. Yeh HW, Hsu EC, Lee SS, et al. PSPC1 mediates TGF-β1 autocrine signalling and Smad2/3 target switching to promote EMT, stemness and metastasis. *Nat Cell Biol.* 2018;20(4):479-491.



- 402 Figure Legends:
- 403 Figure 1. The expressions and correlation of p16, p21, PCNA, and α-SMA in normal oral mucosa
- 404 (NOM) and oral submucous fibrosis (OSF). A-B The representative images of p16, p21, PCNA, and
- 405 α -SMA expressions detected by immunohistochemistry (IHC) in NOM and OSF tissues. C-F
- 406 Quantification of the expressions of p16, p21, PCNA, and α -SMA in NOM and OSF tissues. **G** The
- 407 representative images of lipofuscin expression detected by Sudan Black B staining in the epithelial of
- NOM and OSF tissues (black arrow). H The correlation between p16 and α -SMA expressions in
- 409 NOM and OSF tissues. I The correlation between p16 and PCNA expressions in NOM and OSF
- 410 tissues. J The correlation between p21 and α -SMA expressions in NOM and OSF tissues. K The
- 411 correlation between p21 and PCNA expressions in NOM and OSF tissues. *p < 0.05, **p < 0.01, ***p <
- 412 0.001, and ****p < 0.0001. Scale bar: 100 μ m in 100×, 25 μ m in 400×.

- 414 Figure 2. The performance of senescence-associated beta galactosidase (SA-β-gal) staining, cell
- 415 morphology, and cell proliferation in human oral keratinocytes (HOKs) after senescence
- 416 **induction.** A The representative images of SA-β-gal staining and cell morphology in HOKs treated
- 417 with different concentrations of arecoline (SA-β-gal positive cell: black arrow, green). **B** The
- 418 proportion of SA-β-gal positive cells in HOKs treated with different concentrations of arecoline. C
- 419 Quantification of the surface area of SA-β-gal negative HOKs and SA-β-gal positive HOKs (SA-β-gal
- 420 negative HOK: black arrow, SA-β-gal positive HOK: white arrow). **D** The cell proliferation of HOKs
- treated with different concentrations of arecoline. *p < 0.05, **p < 0.01, **** p < 0.001, **** p < 0.0001.
- 422 Scale bar: 100μm in 100×.

423

- 424 Figure 3. The expression of phosphor-histone H2A.X (γH2A.X) in HOKs treated with different
- concentrations of arecoline after senescence induction. A The representative images of γ H2A.X
- 426 expression in HOKs treated with the different concentrations of arecoline (blue: DAPI, red: γH2A.X,
- 427 γ H2A.X positive cell: white arrow). **B** The proportion of γ H2A.X positive cells in HOKs treated with
- 428 differentiation concentrations of arecoline. C The representative images of the senescent HOK (blue:
- 429 DAPI, red: γH2A.X). *p < 0.05, ** p < 0.01, *** p < 0.001, **** p < 0.0001. Scale bar: 100μm in 100×, 50μm
- 430 in 200×.

431

- 432 Figure 4. The expressions of p16, p21, p53, and TGF-β1 in HOKs treated with 0µg/ml arecoline or
- 433 **320 μg/ml arecoline after senescence induction. A** The representative images of p16, p21, p53, TGF-
- 434 β 1, and GAPDH protein levels in HOKs treated with 0 μ g/ml or 320 μ g/ml arecoline. **B**
- 435 Quantification expressions of p21 at protein and mRNA levels in HOKs treated with 0 µg/ml or 320
- 436 µg/ml arecoline. C Quantification expressions of p53 at protein and mRNA levels in HOKs treated
- with 0 μg/ml or 320 μg/ml arecoline. **D** Quantification expressions of TGF-β1 at protein and mRNA
- levels in HOKs treated with 0 μ g/ml or 320 μ g/ml arecoline. E TGF- β 1 expression in supernatants of
- 439 HOKs treated with 0 μ g/ml or 320 μ g/ml arecoline. *p < 0.05, ** p < 0.01, *** p < 0.001, **** p < 0.0001.

- 441 Figure 5. The mechanism diagram for the role of senescent epithelial cells in the development of
- 442 **OSF.**



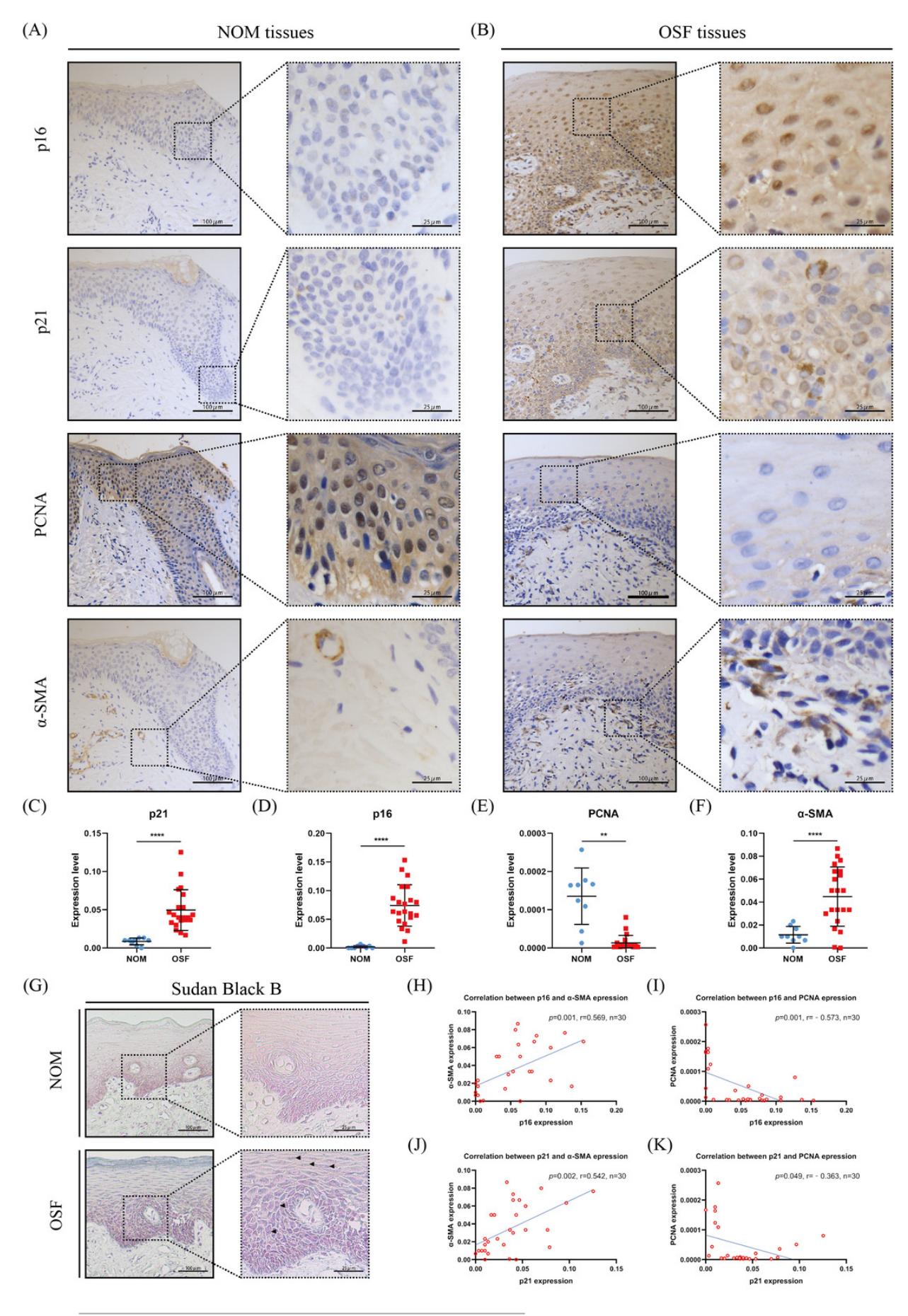
Manuscript to be reviewed

Figure 1

The expressions and correlation of p16, p21, PCNA, and α -SMA in normal oral mucosa (NOM) and oral submucous fibrosis (OSF).

A-B The representative images of p16, p21, PCNA, and α-SMA expressions detected by immunohistochemistry (IHC) in NOM and OSF tissues. **C-F** Quantification of the expressions of p16, p21, PCNA, and α-SMA in NOM and OSF tissues. **G** The representative images of lipofuscin expression detected by Sudan Black B staining in the epithelial of NOM and OSF tissues (black arrow). **H** The correlation between p16 and α-SMA expressions in NOM and OSF tissues. **J** The correlation between p16 and PCNA expressions in NOM and OSF tissues. **J** The correlation between p21 and α-SMA expressions in NOM and OSF tissues. **K** The correlation between p21 and PCNA expressions in NOM and OSF tissues. **K** The correlation between p21 and PCNA expressions in NOM and OSF tissues. *p < 0.05, **p < 0.01, ***p < 0.001, and ****p < 0.0001. Scale bar: 100µm in 100×, 25µm in 400×.





PeerJ reviewing PDF | (2022:11:79139:0:1:CHECK 18 Dec 2022)

Figure 2

The performance of senescence-associated beta galactosidase (SA- β -gal) staining, cell morphology, and cell proliferation in human oral keratinocytes (HOKs) after senescence induction.

A The representative images of SA-β-gal staining and cell morphology in HOKs treated with different concentrations of arecoline (SA-β-gal positive cell: black arrow, green). **B** The proportion of SA-β-gal positive cells in HOKs treated with different concentrations of arecoline. **C** Quantification of the surface area of SA-β-gal negative HOKs and SA-β-gal positive HOKs (SA-β-gal negative HOK: black arrow, SA-β-gal positive HOK: white arrow). **D** The cell proliferation of HOKs treated with different concentrations of arecoline. *p < 0.05, **p < 0.01, **** p < 0.001, **** p < 0.0001. Scale bar: 100μm in 100×.

PeerJ

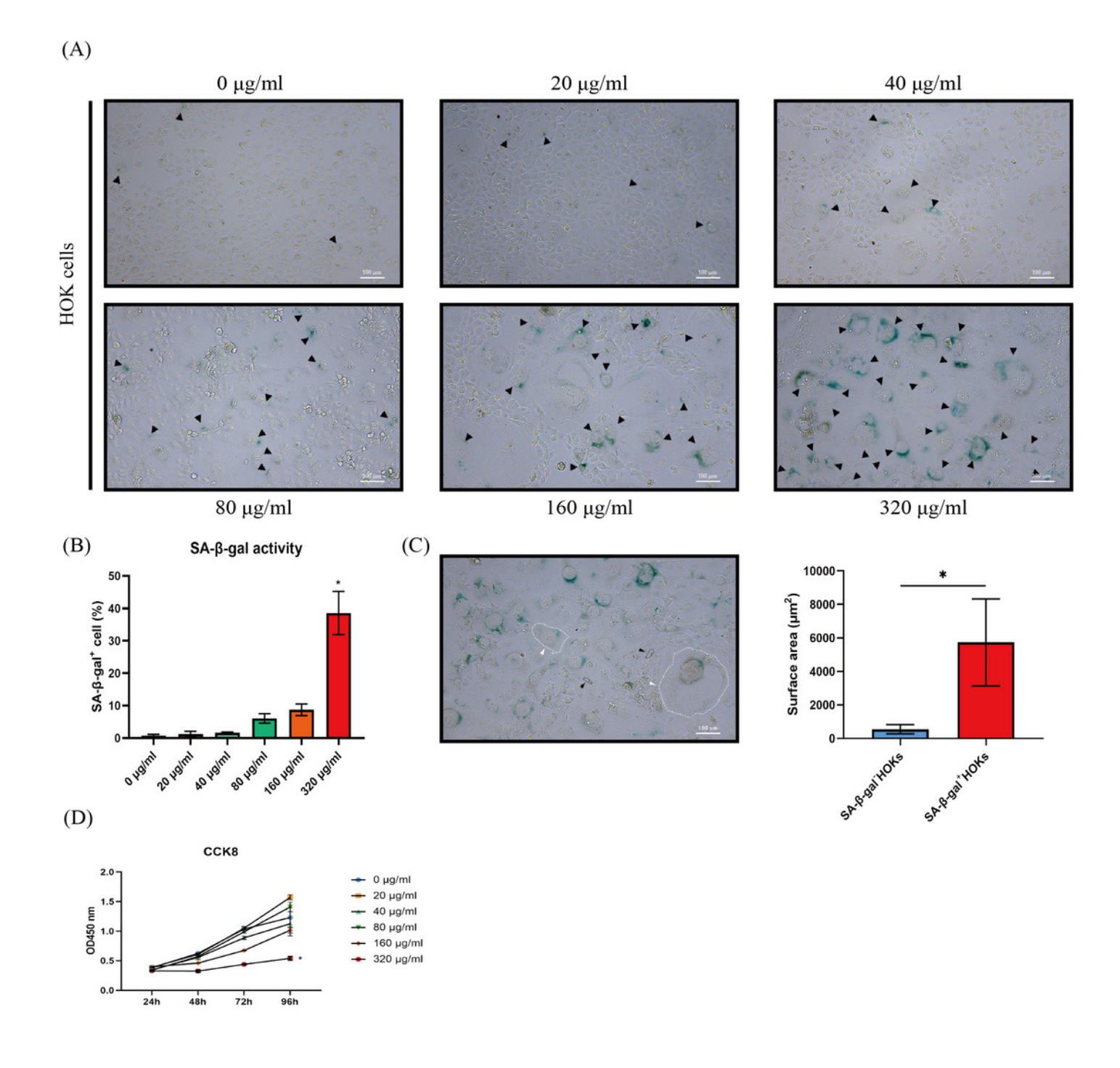


Figure 3

The expression of phosphor-histone H2A.X (γH2A.X) in HOKs treated with different concentrations of arecoline after senescence induction.

A The representative images of γ H2A.X expression in HOKs treated with the different concentrations of arecoline (blue: DAPI, red: γ H2A.X, γ H2A.X positive cell: white arrow). **B** The proportion of γ H2A.X positive cells in HOKs treated with differentiation concentrations of arecoline. **C** The representative images of the senescent HOK (blue: DAPI, red: γ H2A.X). *p < 0.05, ** p < 0.01, *** p < 0.001, **** p < 0.001. Scale bar: 100 μ m in 100×, 50 μ m in 200×.



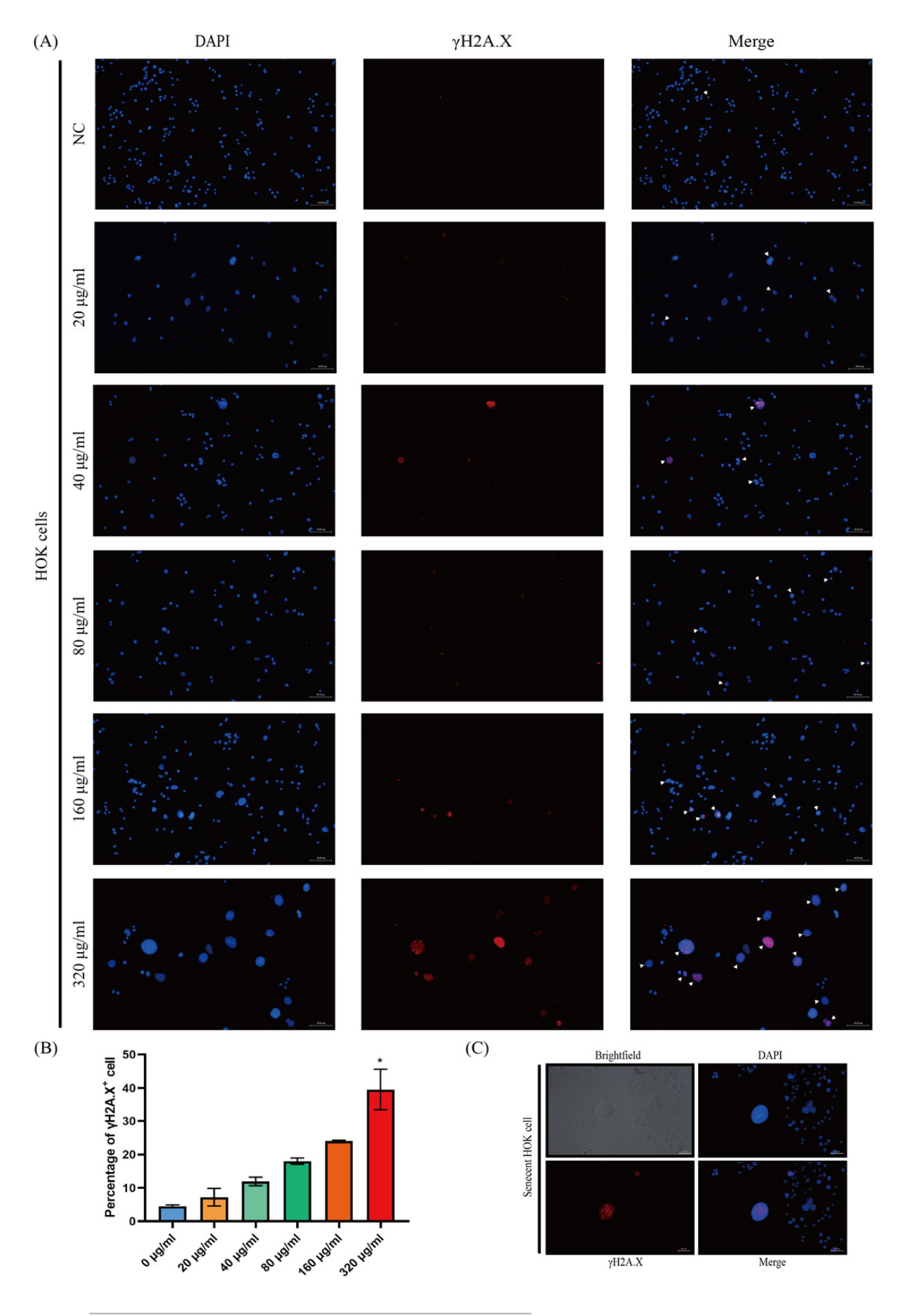


Figure 4

The expressions of p16, p21, p53, and TGF- β 1 in HOKs treated with 0µg/ml arecoline or 320 µg/ml arecoline after senescence induction.

A The representative images of p16, p21, p53, TGF-β1, and GAPDH protein levels in HOKs treated with 0 μg/ml or 320 μg/ml arecoline. **B** Quantification expressions of p21 at protein and mRNA levels in HOKs treated with 0 μg/ml or 320 μg/ml arecoline. **C** Quantification expressions of p53 at protein and mRNA levels in HOKs treated with 0 μg/ml or 320 μg/ml arecoline. **D** Quantification expressions of TGF-β1 at protein and mRNA levels in HOKs treated with 0 μg/ml or 320 μg/ml arecoline. **E** TGF-β1 expression in supernatants of HOKs treated with 0 μg/ml or 320 μg/ml arecoline. *p < 0.05, **p < 0.01, **** p < 0.001.

PeerJ

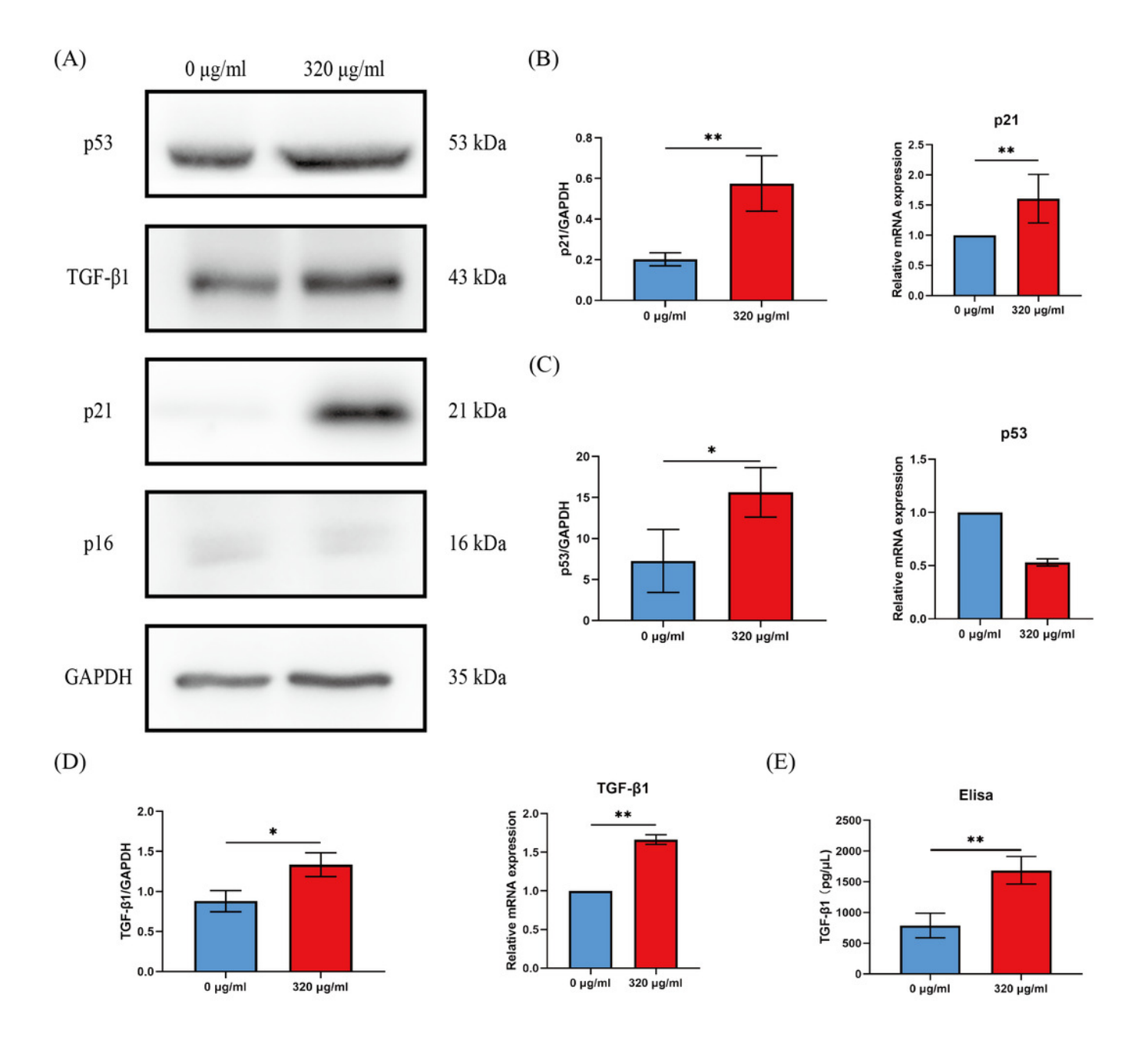




Figure 5

The mechanism diagram for the role of senescent epithelial cells in the development of OSF.

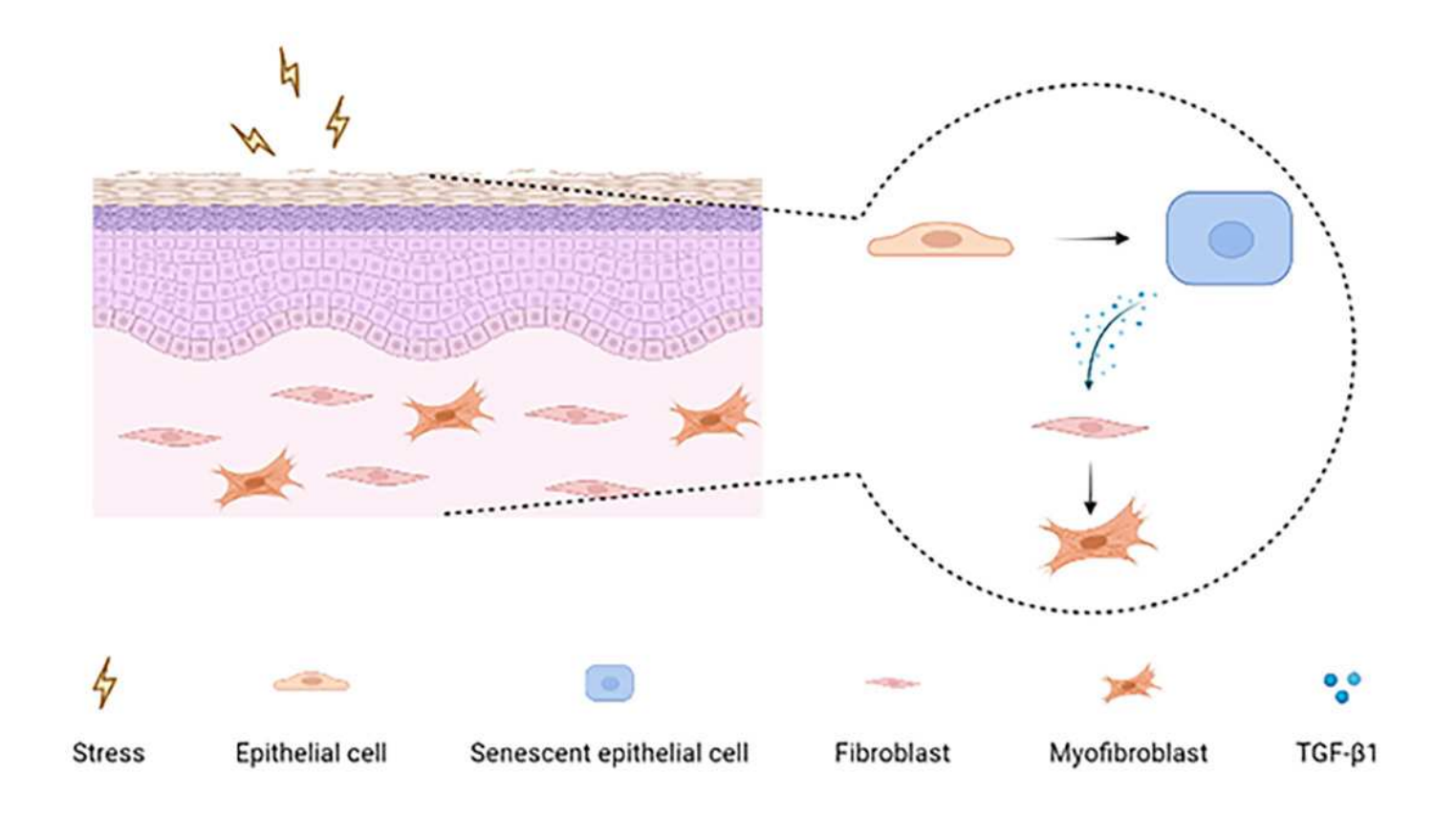




Table 1(on next page)

Primer sequences used in this study



Table 1 Primer sequences used in this study.

Name	Sequence
p16 —	F 5'-GGGTTTTCGTGGTTCACATCC-3'
	R 5'-CTAGACGCTGGCTCCTCAGTA-3'
p21 ——	F 5'-TGTCCGTCAGAACCCATGC-3'
	R 5'-AAAGTCGAAGTTCCATCGCTC-3'
p53 ——	F 5'-CAGCACATGACGGAGGTTGT-3'
	R 5'-TCATCCAAATACTCCACACGC-3'
TGF-β1 ——	F 5'-CTAATGGTGGAAACCCACAACG-3'
	R 5'-TATCGCCAGGAATTGTTGCTG-3'
GAPDH —	F 5'-CCATGGGTGGAATCATATTGGA-3'
	R 5'-TCAACGGATTTGGTCGTATTGG-3'